

Proton Transport, An Examination of Model and Experimental Data For Space Environment Protons

By P. Layton, L. Adams, D. Krawzsenek, B. Passenheim, J. Pickel
Maxwell Technologies Microelectronics and Spur Electron/Brunel University

Introduction

In the last decade the space community has seen a change from the dominance of a few countries with a focus on military applications to a worldwide involvement of an increasingly commercial nature. Similarly, the components used in satellites have evolved increasingly from the traditional radiation hardened components to the use of commercial silicon electronics. Using commercial electronics requires radiation characterization and generally some form of radiation analysis and mitigation for the intended application. In this case the satellite designer is trading the known radiation tolerance characteristics of a radiation hardened IC for the higher performance and lower cost of a commercial IC.

One of the principal mitigation schemes for total ionizing dose (TID) involves using a combination of analysis of the radiation environment and part placement in the satellite with shielding at the part level. In this case, the orbital radiation environment is modeled to produce a dose versus shielding depth analysis. The intended ICs are characterized by TID testing, typically using gamma radiation from a Co-60 source. Generally an estimated satellite shielding is then used to determine if the IC will meet the mission requirement using the dose-depth curve.

At this point the part will either meet the mission requirement or will require additional radiation mitigation. The mitigation approach discussed in this paper is the use of localized shielding. Shielding can be used in a variety of ways. There is shielding from the satellite skin, box level shielding, other components and finally part level shielding. A component can be placed deep inside a satellite, using other components and systems for shielding. Unfortunately, the satellite is usually not completely received increased interest recently because of the desire by many of the planned satellite constellations to fly in the proton belts and the question of solar flare survival in all orbits. This paper will address the effectiveness of shielding against protons. Of particular interest is the effectiveness of shielding radiation down to levels that are within the tolerance of commercial ICs. Although the effectiveness of shielding electrons will briefly be discussed in reference to the total ionizing dose behind an amount of shielding, the principal focus will be on protons.

For package-level shielding, physical space is particularly limited. There is an advantage for using high-Z material for localized shielding, compared to standard material such as Al or Kovar, because of the increased density and consequent increased effective shielding thickness for a given thickness. The shielding effectiveness of high-Z material for electrons is well established. In the space environment, energetic protons are also a major contributor to ionizing dose, as well as displacement damage. While the shielding improvement for high-Z material is not as large for protons as for electrons, there is nonetheless significant improvement. For example, in a 2000 km circular orbit with 60 degree inclination, the severe

proton environment from the trapped belts would result in a dose to Si of 9.49E5 rad(Si) per year for a thin shield of 1 mm Al. For a 100 mil Al shield, the annual dose is reduced to 3.14E4 rad(Si) and for 100 mil W shield the dose is 1.35E4 rad(Si), a reduction by a factor of 0.43.

Modeling

The shielding improvement is due primarily to two factors; 1) proton stopping power (in terms of energy loss per path length) is larger in high-Z material compared to low-Z material and 2) more high-Z material can be utilized in a given thickness because of the higher density. Figure 1(a) shows the stopping power of protons in Al versus proton energy and Figure 1(b) compares the stopping power in W to stopping power in Al. The stopping power is higher in W than in Al by a factor of 3 to 5 in the energy range of protons that reach the interior of the spacecraft. Consequently, fewer protons will reach the target Si die for the high-Z shield as compared to an aluminum shield of the same thickness.

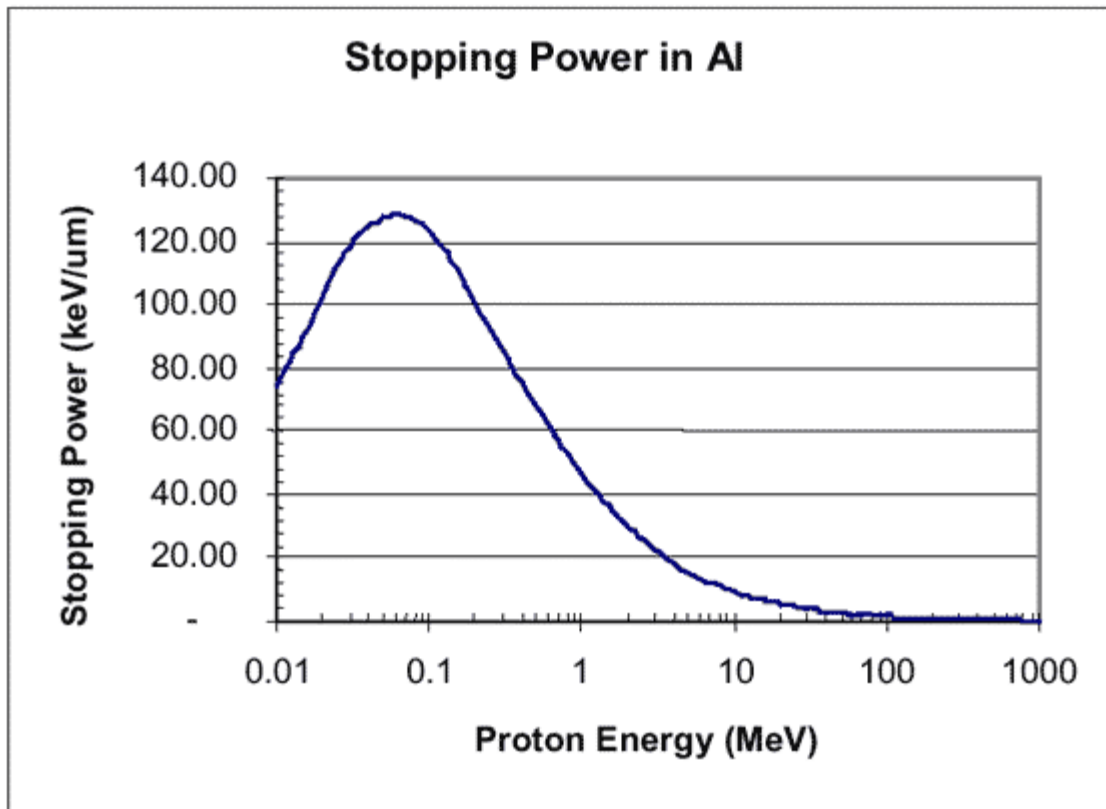


Figure 1(a): Proton stopping power versus energy in Al

As proton energy decreases, stopping power increases through the Bragg peak, as illustrated in Figure 1(a). However, the average energy of the proton spectra increases with increasing shield thickness. Figure 2 shows the proton spectra at a target transported through three different levels of shielding in a orbit of 2000km circular at a 60 degree inclination. This orbit is in the middle trapped proton belt, and is one of the most difficult orbits to shield. The three shield levels are 1), a nearly

unshielded target of 1 mil Al 2), a lightly shielded target of 100 mils of Al and 3), a high-Z shielded target using 100 mils of W.

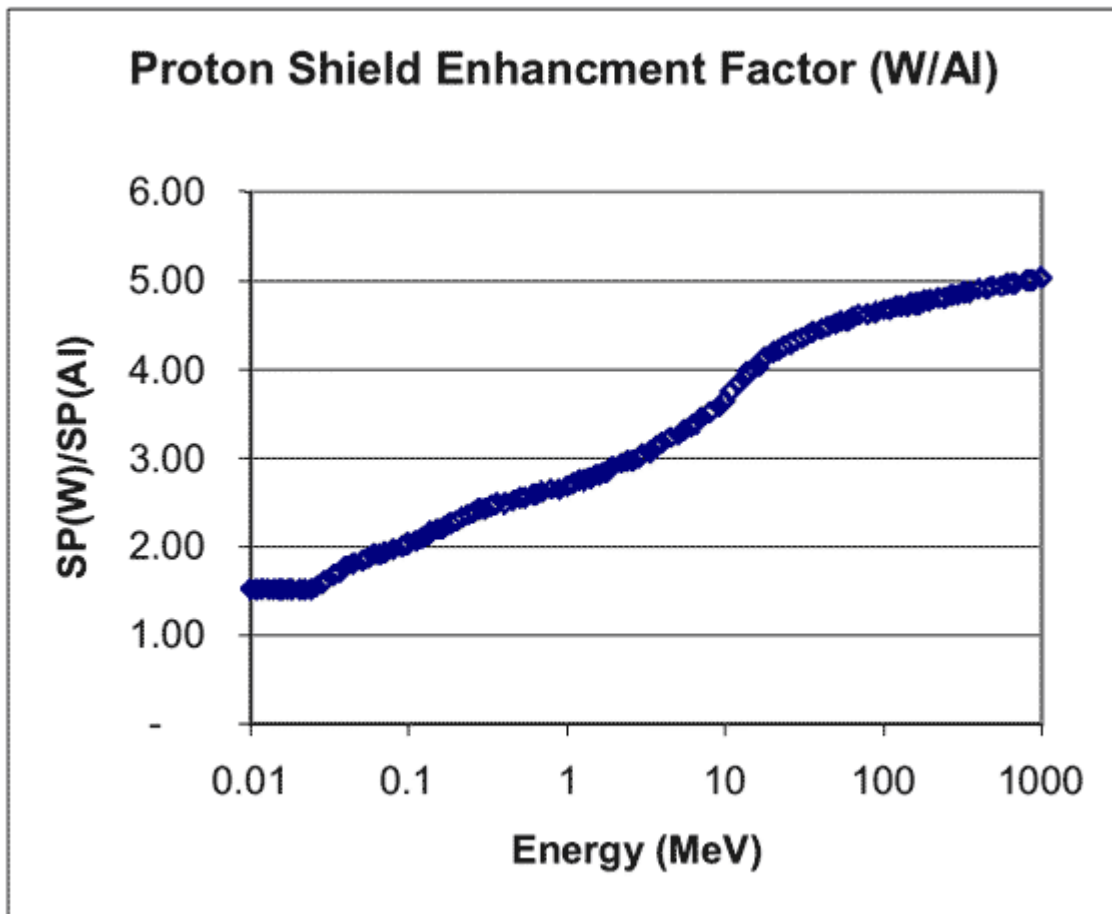


Figure 1(b): Ratio of proton stopping power in W to Al versus energy

As proton energy decreases, stopping power increases through the Bragg peak, as illustrated in Figure 1(a). However, the average energy of the proton spectra increases with increasing shield thickness. Figure 2 shows the proton spectra at a target transported through three different levels of shielding in a orbit of 2000km circular at a 60 degree inclination. This orbit is in the middle trapped proton belt, and is one of the most difficult orbits to shield. The three shield levels are 1), a nearly unshielded target of 1 mil Al 2), a lightly shielded target of 100 mils of Al and 3), a high-Z shielded target using 100 mils of W.

For the high-Z case, we see a hardening of the spectrum and fewer protons in the lower energy range. The reduction of protons in the lower energy range is an important factor in the effectiveness of shielding since the stopping power in the target (Si) increases at lower energy.

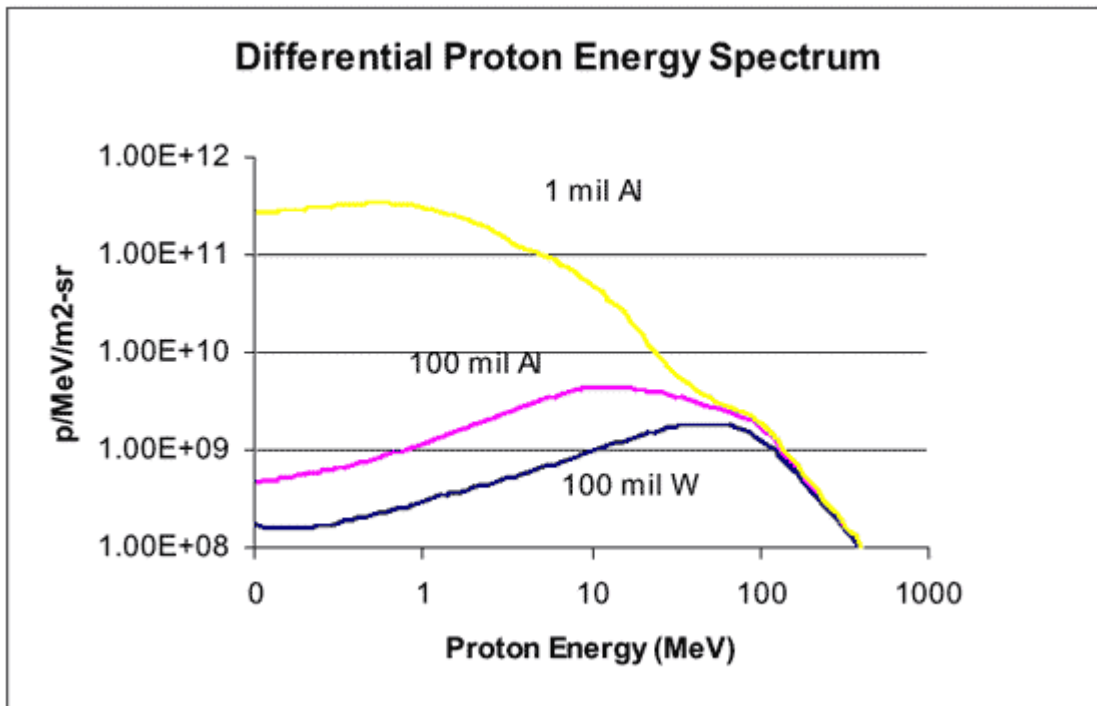


Figure 2: Proton energy spectra for protons at 2000 km x 2000 km, 60 degree orbit behind various shields.

Previous papers show the effects of mono-energetic protons on Maxwell Technologies RAD-PAK™ package [1,3,4]. It is important to note that space radiation is not mono-energetic and is effectively isotropic in most cases. Therefore, two effects occur that increase the effectiveness of localized package-level shielding: 1) the slant range effect and 2) the prevalence of lower energy protons over higher energy protons. The end result is a lower total dose with increased shielding thickness.

An additional shielding consideration is the isotropic nature of protons in space. The slant range due to isotropic proton incidence (1/cos.σ effect) results in higher effective shield thickness for most of the incident protons.

A sample proton fluence versus energy spectrum is shown in Figure 3 for an orbit of 1457 km and 55 degrees inclination. This case is for an early Skybridge orbit, which lies within the proton belts. Note; this is no longer the current Skybridge orbit, but it is very close to the current orbit of 1469 km at 53 degrees inclination. The three curves show proton fluence vs. energy, and the annual ionizing dose, for three cases: outside the spacecraft (no shielding); through a thin space-craft wall of 1 mm; and through the space-craft wall plus 1.25 mm Al component box plus Maxwell's thinnest RAD-PAK™ package.

The lower energy protons (<10 MeV) are the primary constituents of the proton spectrum. It can be seen that although 1 mm of Al attenuates the lower energy proton component and reduces the dose by 3 orders of magnitude, additional shielding, represented by the RP1 case, reduces the total-dose further. In shielding

commercial electronics, small improvements in shielding effectiveness often make the difference between part acceptance and rejection.

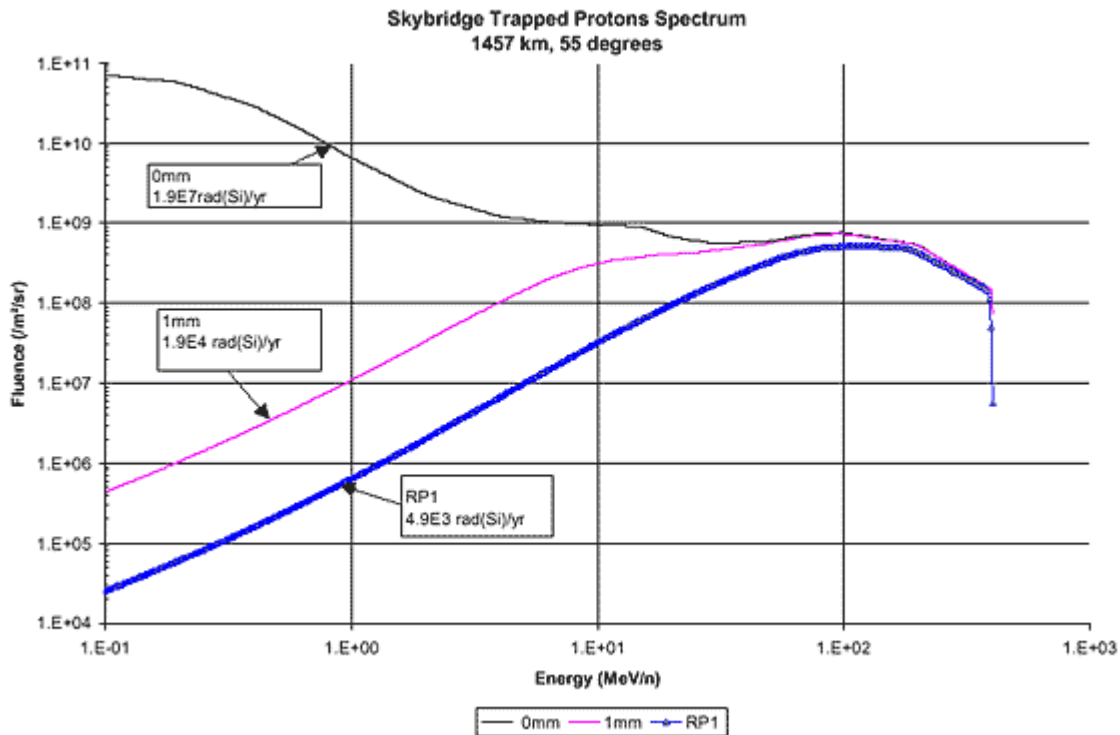


Figure 3: Proton energy spectra and annual dose for various shields in a typical orbit within the proton belts.

For example, a typical commercial 4 Meg SRAM has an intrinsic die tolerance of 10 to 40 krad(Si). For an 8 year mission, none of the SRAMs with minimal 1 mm shielding would survive beyond approximately two years of the mission. Yet behind shielding, represented by RP1, the 40 krad(Si) tolerance case would survive the entire 8 years mission, or 4 times longer than the device with 1 mm shielding. This simple analysis does not take into consideration the isotropic nature of radiation through packaging. Here, through the lid and the base, there is an additional amount of shielding proportional to $1/\cos(\alpha)$ times the shielding thickness, where α is the incident angle of the proton on the packages.

This increase in effective shielding can be seen by comparing a spherical shell model versus a slab model. Using the CRRES orbit as an example, there is approximately a 3.6 times increase in the effective shielding when using a slab model as compared to a spherical shell model. This can be seen in table 1(a) which compares two different modeling programs for the CRRES orbit for Solar Min. Table 1(a) shows a comparison of a 2π model using Space Radiation 4.0 with a finite slab model generated by Space Environment Analyst (SEA). This analysis shows an approximate 3.6x average improvement.

Proton Data dose in rad(Si)

	10 mils Al	100 mils Al	1000 mils Al
Space Radiation 4.0 (spherical)	7.01E+05	8.64E+03	6.46E+02
Space Environment Analysis (slab)	2.18E+05	2.18E+03	1.74E+02

Table 1(a): Comparison of Slab to 2π Shielding

Proton Data dose in rad(Si)

	10 mils Al	100 mils Al	1000 mils Al
Space Radiation 4.0	7.01E+05	8.64E+03	6.46E+02
Space Environment Analysis	6.53E+05	6.53E+03	4.35E+02

Table 1(b): Comparison of SEA code to Space Radiation 4.0 for 2π models

Table 1(b) shows a comparison of the two programs (SEA and Space Radiation 4.0) using a 2π analysis for both. When using the spherical geometry, the two models deviate by less than 10% for minimal amounts of shielding and less than 50% for higher amounts of shielding (one inch). In summary, when using the finite slab geometry there is more effective shielding than using spherical geometry. This geometrical distinction plays to the advantage of shielded packages.

CRRES Flight Data

An early demonstration of the effectiveness of shielding was demonstrated on the CRRES Microelectronics Test Package (MEP)⁵. Figure 4 [5] shows the dose received per orbit for various levels of shielding. The sharp rise on orbit 588 shows a major Solar Particle Event (SPE) that occurred on 24 March 1991. The levels correspond to dosimeters placed on boards with microelectronics placed on them. The outermost board (level 1), had 10 mils aluminum plus the shielding for the lids of the parts, level 2 had the additional shielding provided by the fully loaded board from level 1, and level three had the additional shielding provided by the fully loaded boards from level 1 and 2.

The total dose received on each dosimeter for the various levels of shielding are: 165 krad (Si) at board level 1, 9.2 krad(Si) at board level 2, 2.5krad(Si) at board level 3, and 0.665 krad(Si) through the RAD-PAK™ package on board level 1. A dosimeter was placed inside the RAD-PAK™ package and showed two and a half orders of magnitude improvement over the unshielded dosimeters at level 1.

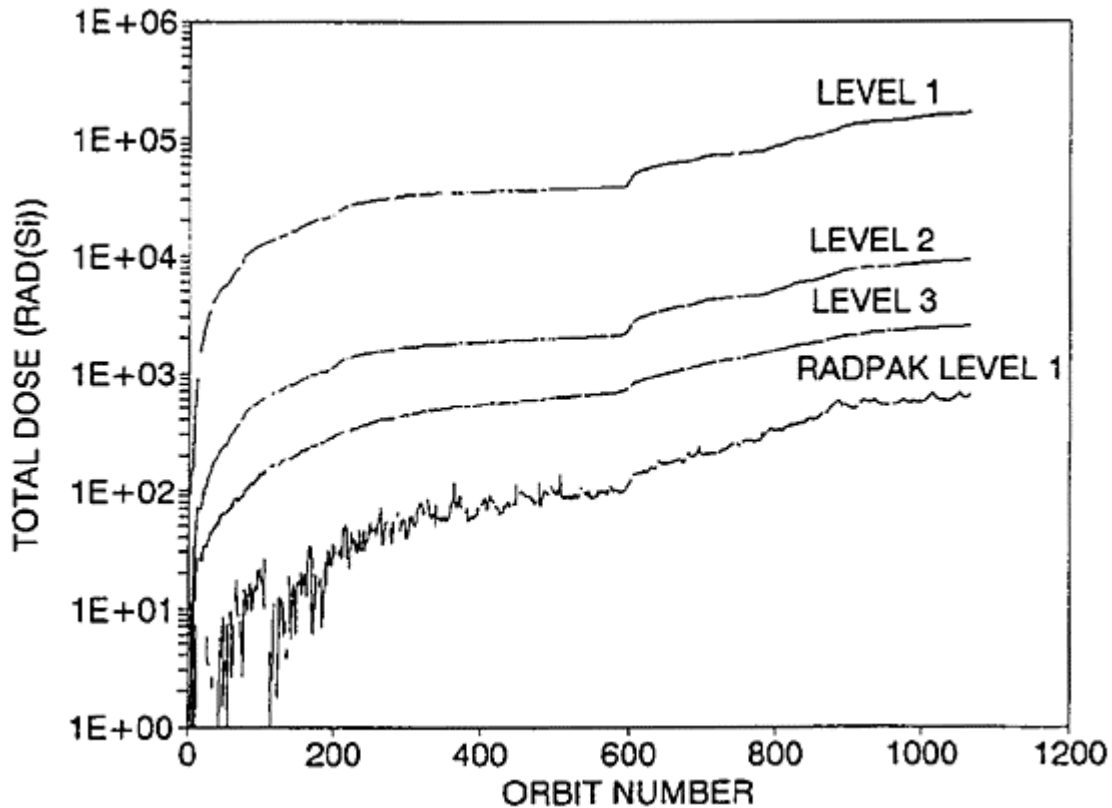


Figure 4: CRRES data, dose versus orbit for various shielding levels.
Courtesy of Mullen et al. [5]

CRRES used spherical half domes with varying degrees of shielding in front of a dosimeter to measure time varying radiation levels and to correlate to the board level shielding. This was used to correlate the total dose to the amount of shielding in front of boards with microelectronics on them. The boards also had dosimeters. The spherical dome's dosimeter data correlated well to the board dosimeters for each corresponding level. The dosimeters on Dome 1, with 82.5 mils Al, correlated to dosimeters for board level 1. Dome 2, with 232 mil Al, correlated to board level 2. Dome 4, with 886.5 mil Al, correlated to board level 3. [7].

Figure 5 shows a dose depth curve of the CRRES orbit of 33500 km by 350 km at 18.1 degree inclination, calculated using space radiation 4.0. The plot shows trapped protons, electrons and solar protons over 1 year period and a 14.4 month period. There were 1067 orbits with an orbit period of approximately 590 minutes.

CRRES Solar Min 33,500km x 350km 18.1 degrees

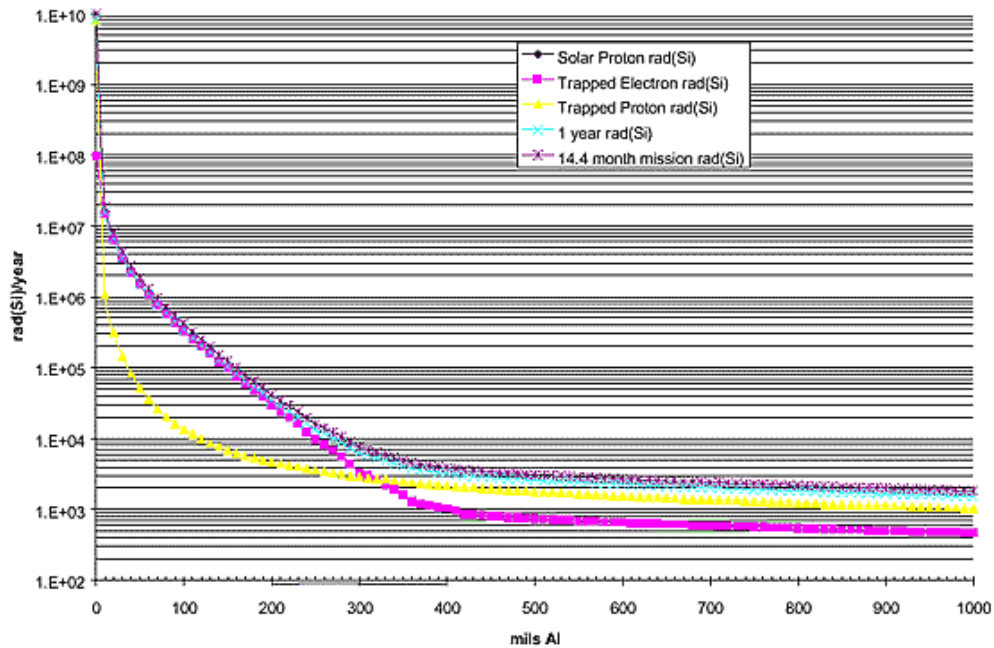


Figure 5: CRRES dose versus depth in mils Al model using Space Radiation 4.0

COMPARISON OF TOTAL DOSE PREDICTIONS WITH SRD DATA
FOR ENTIRE MISSION DURATION
18 DEG, H=350/33000KM, SOLAR MAXIMUM

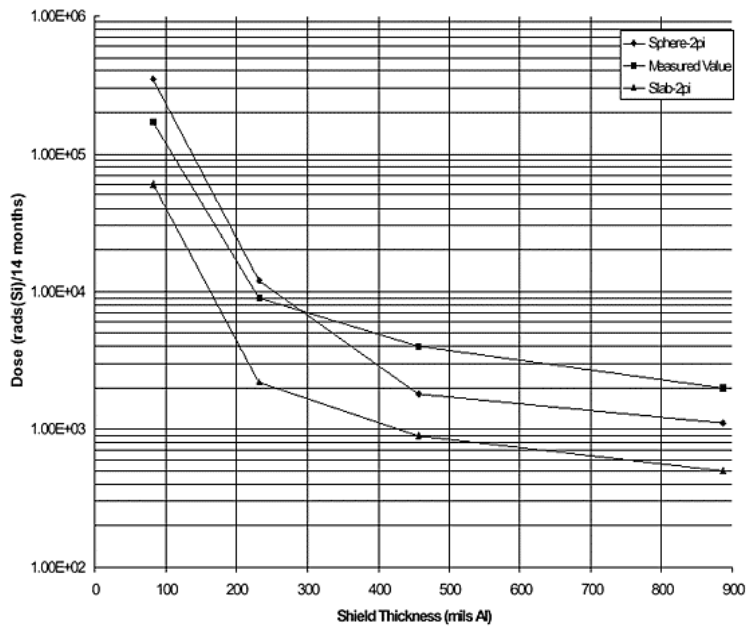


Figure 6: NASA data showing 2π slab shielding and CRRES measured data. Courtesy of NASA [9]

Figure 6 is a dose depth curve of the CRRES orbit, showing the two different geometries as discussed above, as well as showing the actual measured values. This graph was taken from a NASA technical paper [9].

Reference [7] has an in-depth discussion of the time and spatial variation of the total dose measured on the CRRES satellite. To compare with model data Space Radiation 4.0 was used which incorporates the AE8 and AP8 models for trapped electrons and trapped protons respectively. Using the model, the CRRES environment is dominated by trapped electrons for shielding less than 300 mils aluminum, after that the trapped protons dominate the spectrum. Table 2 below shows a comparison of actual to predicted data.

It appears that for lessor amounts of shielding, the model over estimates the amount of total dose. In the higher shielded realm, shown under level 2 and 3, the numbers are much closer. With this amount of shielding, the trapped protons are the dominant species, therefore it is reasonable to assume that there is good correlation of the actual CRRES proton spectrum to the model. Since trapped electrons are the dominant species for shielding less than 300 mils Al, it appears that the AE8 model over predicts the trapped electron spectrum for the CRRES orbit.

	Amount of shielding Mils Al	CRRES Measured dose krad(Si)	Predicted dose Space Radiation 4.0 krad(Si)
Level 1	82.5	165	335
Level 2	232	9.2	11.5
Level 3	886.5	2.5	1
RAD-PAK		0.665	

Table 2: Comparison of CRRES data and predicted dose

The dosimeter in the RAD-PAK™ package, measured 665 rad(Si). This corresponds to shielding of greater than one inch of Al. The actual dosimeter was shielded by only 10 mils aluminum plus the RAD-PAK™ package. This shows that even in the proton dominated realm of greater than 300 mils Al shielding, that the RAD-PAK™ package effectively shields the device from protons. Using a straight density equivalence of the RAD-PAK™ package and using a slab shield geometry, as explained above in the modeling section (II), yields an effective shielding less than the level 3 board. In that case one would expect 2500 rad(Si), instead of the 665 rad(Si) that was measured inside of the RAD-PAK™ package. We are unable to explain why the dose measured inside the RAD-PAK™ package was so low. The dosimeter was functioning, since the data from dosimeter in the RAD-PAK™ package tracked well to the dosimeters on the other board levels as shown in figure 4 above.

MIR Flight Data

Dose measurements from the REM instrument on-board the MIR spacecraft were compared to calculations of proton and electron dose using embedded codes within the Space Radiation code.

The REM instrument contains two Si detectors that measure energy loss spectra of charged particles behind shields of 0.7 mm Al (designated the electron detector) and 3 mm of Al plus 0.75 mm of Ta (designated the proton detector), respectively [8]. The electron detector sees both protons and electrons. The proton detector sees mostly protons since the extra 0.75 mm Ta effectively reduces penetration of electrons in the relevant energy range.

The instrument was mounted externally to MIR and monitored from Nov. 94 until Feb. 96. The main aperture for both the proton detector and the electron detector is defined by an Al cone. The opening to the detectors is 90 degrees. The sides of the detectors and the backside are shielded by a minimum of two inches of material. The shielding along the sides and behind the detectors effectively blocks out any electrons, leaving the detectors open to 14.6% of the electron environment surrounding it.

In Space Radiation 4.0, the calculated electron dose values are for the entire spherical shell. These values were then multiplied by the factor 0.146 to represent the detectors visibility. This however is not the case for protons. The dose depth curve for protons, as calculated with Space Radiation 4.0, goes relatively flat after 5mm of shielding. With this in mind, the model calculations represented here for protons takes into account the 14.6% of visible space through the dome shielding, and then uses 1 inch Al of shielding for the remaining 85.4% of space. The MIR orbit is circular at ~400 km altitude and 52 degrees inclination. The dose was mainly accumulated in two regions, the South Atlantic Anomaly (SAA), due primarily to protons, and the region of closest approach to the magnetic poles (designated Non-SAA), due primarily to electrons.

Average daily dose measurements from reference 8 were compared to calculations generated using Space Radiation 4.0 as shown in Table 3. To simplify the calculation, we assumed that the proton dose is delivered only in the SAA region and the electron dose is delivered only in the Non-SAA region. We arrived at this assumption by comparing the proton detector to the electron detector for both regions. In the Non-SAA region the additional shielding from the proton detector shows that the majority of the dose came from easily shielded electrons. In the SAA region, the higher P/E ratio shows that the particles were harder to shield suggesting that they are primarily protons.

The Space Radiation 4.0 calculations for dose are the average over the entire orbit. For the SAA region, calculations were performed for protons only, and for the Non-SAA region the calculations were performed for electrons only. Since Space Radiation cannot perform Ta transport calculations in combination with Al calculations, we converted the Ta to equivalent mm of Al. Reference 8 gives us the proton equivalent to 0.75mm of Ta as well as the electron equivalent to 0.75mm of Ta, these are 2.9mm Al and 3.6mm Al respectfully. In other words, for the proton detector we used 5.9mm (2.9mm + 3mm) of Al shielding in the case of protons and in the case of electrons we used 6.6mm (3.6mm + 3mm) of Al shielding.

Table 3 shows the REM data compared to model calculations. The model calculations show both Solar Min and Solar Max. The electron calculations (Non-SAA) are an average of 2.0 times lower than measurements for the proton detector and 5.3 times higher for the electron detector. Also in this region, the calculated P/E ratio is an average factor of 5.8 lower than the MIR data, suggesting that the electron model (AE8) is over predicting the electron fluence. In the SAA region we have a very good agreement with the P/E ratio, with the Solar Min off by only 0.4%. In both Solar Min and Solar Max the P/E ratio for the proton dominated environment showed a good agreement between the calculations and the REM measurements. This suggests that the AP8 model is relatively accurate in this region of space.

The calculations and the measurements demonstrate that adding the extra layer of high-Z shielding lowered the total dose at the detector. Based on the REM data the proton dose was reduced by ~20% to 30% and the electron dose was reduced by ~96% to 97%.

	REM			Calculations		
	P det	E det	P/E	P det	E det	P/E
Solar Max	75	110	0.68	37	45	0.822
SAA						
Solar Min				65	96	0.677
Solar Max	5.1	150	0.034	5.5	1168	0.005
Non SAA						
Solar Min				2.8	420	0.007

Table 3: Average daily dose (mrad(Si)) measurements from REM on-board MIR compared to code calculations

Detectors in general

Generally high Z materials are used for detectors to screen out electrons and to discriminate proton energies. In Reference [6], an omnidirectional detector was designed using Al, Cu and W as shields to set threshold energies for protons and electrons for the TIROS/NOAA low altitude weather satellites. Additional flight data can be derived from these results.

The UK mini-satellite program STRV-1c/d, scheduled to fly in early 2000, has a controlled flight experiment that will be used to validate RAD-PAK™ and RAD-COAT shielding technologies. This data will compare non-shielded (RADFETS) detectors to shielded detectors and components. The data from this satellite will be used to analyze the effects of integrated shielding, slab shielding and the use of high Z shielding.

We have looked at both experimental and predicted data based on models for the effectiveness of shielding protons in the space environment. With both forms of analysis, shielding lowers the total dose received at the die. As can be seen by the

data, high Z shielding is more effective than aluminum of the same thickness. Also, the geometry of the shielding is important. Since space radiation is on average isotropic, there is an additional benefit proportional to $1/\cos\theta$ times the shielding thickness for each incident particle.

The shield effectiveness is also dependent on the distance from the die to the shield. For slab shields, the further the shield is from the die, the greater the side leakage. Therefore packages with integrated shielding (like RAD-PAK™) are the most effective shielding both for minimizing weight and the size of shielding required.

Acknowledgments

The authors wish to thank Gerry Gurtman and Mel Rice and Maxwell Technologies for their support in performing TRIM calculations and analysis. Also, we thank Gary Mullen and Susan Gussenhoven for their support with CRRES information.

References

- [1]. J.P. Spratt, B.C. Passenheim, R.E. Leadon, S. Clark, and D.J. Strobel, "Effectiveness of IC Shielded Packages Against Space Radiation", IEEE Trans. Nucl. Sci., Vol 44 pp2018 – 2025, 1997.
- [2]. G.F. MacKay, I. Thomspson, L. Adams, R. Nickson, A. Ng, and N. Sultan, "An Instrument for Monitoring Proton-Induced Upsets in Space Electronics", RADECS 1997, IEEE 97TH 8294 , pp495-498.
- [3]. L. Adams, R. Nickson, A. Kelleher, D.G. Millward, D. J. Strobel, D. Czajkowski, "A dosimetric Evaluation of the RAD-PAK™ Using Mono-Energetic Electrons and Protons" RADECS 1995, IEEE 95TH8147, pp. 449-452.
- [4].D.G. Millward, D. J. Strobel, "The Effectiveness of RAD-PAK™ ICs for Space Radiation Hardening", Proc. Of 40th ECTC conference, Los Vegas, May 1990.
- [5] E.G. Mullen, K.P. Ray, " CRRES Microelectronics Test Package (MEP), IEEE Trans. Nucl. Sci. , Vol. 40, No. 2, April 1993.
- [6] S.L. Huston and K.A. Pfitzer "A New Model for the Low Altitude Trapped Proton Environment" IEEE Trans. Nucl. Sci, Vol. 45, No. 6, December 1998, pp. 2972-2978.
- [7] E.G. Mullen, M.S. Gussenhoven, D.H. Brautigam, and A.R. Frederickson, "Review of CRRES Radiation Belt Measurements and Engineering Experiment Results", SAEI 22nd international Conference on Environmental Systems, July 1992, paper no. 921373.
- [8] P. Buhler, L. Desorgher, A. Zehnder, E. Daly, and L. Adams, "Observations of the Low Earth Orbit Radiation Environment from MIR," Radiation Measurement, 26, 917-921 (1996).
- [9] E.G. Stassinopoulous, G.J. Bruker, and C.A. Stauffer, "CRRES Micro-Electronics Package Flight Data Analysis" NASA Technical Paper 3423, June 1993.